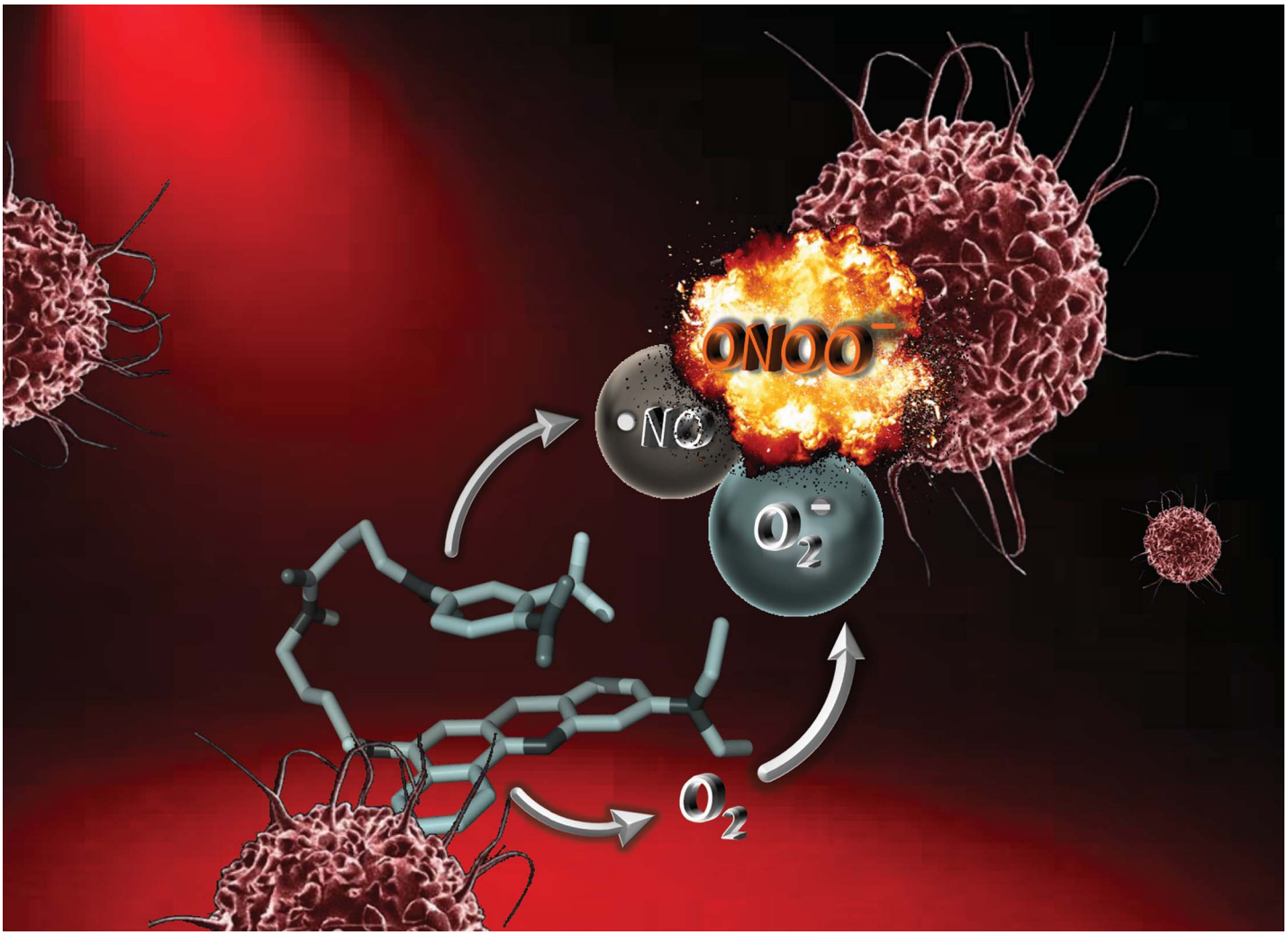

Showcasing collaborative research from Professor Sortino's laboratory, Department of Drug and Health Science, University of Catania (Italy), Department of Drug and Science Technology, University of Torino (Italy) and Department of Biology, University of Padova (Italy).

A generator of peroxynitrite activatable with red light

We have developed a molecular hybrid able to generate the cytotoxic peroxynitrite with the highly biocompatible and tissue penetrating red light. Besides, the fluorescence of the hybrid allows its tracking in different types of cancer cells where it is well-tolerated in the dark but induces a remarkable cell mortality under light irradiation in a very low concentration range, with very low light doses. In view of these properties, the presented compound can open up intriguing prospects in biomedical research, where precise and spatiotemporally controlled concentrations of $ONOO^-$ are required.

As featured in:

See Loretta Lazzarato, Salvatore Sortino *et al.*, *Chem. Sci.*, 2021, **12**, 4740.

ROYAL SOCIETY OF CHEMISTRY

rsc.li/chemical-science

Registered charity number: 207890

Chemical Science

ROYAL SOCIETY OF CHEMISTRY

EDGE ARTICLE

View Article Online
View Journal | View Issue

Cite this: *Chem. Sci.*, 2021, **12**, 4740

All publication charges for this article have been paid for by the Royal Society of Chemistry

A generator of peroxynitrite activatable with red light†

Cristina Parisi, ‡[a] Mariacristina Failla, ‡[b] Aurore Fraix, ‡[a] Luca Menilli,[c] Francesca Moret,[c] Elena Reddi,[c] Barbara Rolando,[b] Francesca Spyrakis,[b] Loretta Lazzarato, *[b] Roberta Fruttero,[b] Alberto Gasco[b] and Salvatore Sortino *[a]

The generation of reactive oxygen species (ROS) and reactive nitrogen species (RNS) as "unconventional" therapeutics with precise spatiotemporal control by using light stimuli may open entirely new horizons for innovative therapeutic modalities. Among ROS and RNS, peroxynitrite ($ONOO^-$) plays a dominant role in chemistry and biology in view of its potent oxidizing power and cytotoxic action. We have designed and synthesized a molecular hybrid based on benzophenothiazine as a red light-harvesting antenna joined to an *N*-nitroso appendage through a flexible spacer. Single photon red light excitation of this molecular construct triggers the release of nitric oxide ($^{\bullet}NO$) and simultaneously produces superoxide anions ($O_2^{\bullet-}$). The diffusion-controlled reaction between these two radical species generates $ONOO^-$, as confirmed by the use of fluorescein-boronate as a highly selective chemical probe. Besides, the red fluorescence of the hybrid allows its tracking in different types of cancer cells where it is well-tolerated in the dark but induces remarkable cell mortality under irradiation with red light in a very low concentration range, with very low light doses (*ca.* 1 J cm^{-2}). This $ONOO^-$ generator activatable by highly biocompatible and tissue penetrating single photon red light can open up intriguing prospects in biomedical research, where precise and spatiotemporally controlled concentrations of $ONOO^-$ are required.

Received 22nd December 2020
Accepted 3rd March 2021

DOI: 10.1039/d0sc06970a

rsc.li/chemical-science

Introduction

Peroxynitrite ($ONOO^-$) is a reactive nitrogen species (RNS) with a half-life of 1.9 s at pH 7.4, arising from the diffusion-controlled reaction between nitric oxide ($^{\bullet}NO$) and the superoxide anion ($O_2^{\bullet-}$) ($k \sim 10^{10}$ M^{-1} s^{-1}).[1] $ONOO^-$ is simultaneously a potent oxidant and a nucleophile and these features determine its fate in a biological environment.[2] In particular, $ONOO^-$ is in equilibrium with its conjugate acid, ONOOH (pK_a = 6.8),[3] which may either isomerize (~70%) or undergo homolytic cleavage to produce $^{\bullet}OH$ and $^{\bullet}NO_2$ radicals (~30%)[4] which are, in turn, mainly responsible for its oxidizing and nitrating activity.[5] In view of this double ability to act as a nucleophile and generator of very reactive secondary free radical species, $ONOO^-$ is labelled as a strong cytotoxic agent.[6] Analogously to singlet oxygen ($^1O_2$), the ROS playing a dominant role in photodynamic therapy,[7] $ONOO^-$ is a multitarget cytotoxic agent able to react with lipids, DNA, and proteins as demonstrated by its short biological half-life (<20 ms).[2,4,5] However, in contrast to $^1O_2$, $ONOO^-$ offers the additional advantage of radical-mediated nitration of the protein tyrosines,[5,8] a process at the basis of the inhibition of the cell efflux pumps mainly responsible for multidrug resistance (MDR).[9] As a consequence, $ONOO^-$ can be exploited not only as a cytotoxic agent but also as a powerful tool to reduce the cell extrusion of conventional chemotherapeutics, and thus enhancing their anticancer activity.[10]

This scenario makes molecules able to generate $ONOO^-$ potential anticancer prodrugs. However, due to the lack of selectivity of $ONOO^-$ for bio-substrates, precise spatiotemporal control in the $ONOO^-$ delivery is highly desirable in view of practical applications. Light represents a powerful remote activation tool in this regard, offering high potential for innovative "unconventional" therapeutic approaches, which can open entirely new horizons in cancer treatment.[11] Photons are in fact ideal external stimuli for the rapid introduction of cytotoxic agents at the target site starting from appropriate photoprecursors, mimicking an "optical syringe" with superb control of sites, time and dosage of the released species, all these factors being determining for a positive therapeutic outcome. Moreover, light-triggering provides the unique advantage of not altering the physiological values of

[a]*PhotoChemLab, Department of Drug and Health Sciences, University of Catania, I-95125, Italy. E-mail: ssortino@unict.it*

[b]*Department of Science and Drug Technology, University of Torino, I-10125 Torino, Italy. E-mail: Loretta.lazzarato@unito.it*

[c]*Department of Biology, University of Padova, I-35131 Padova, Italy*

† Electronic supplementary information (ESI) available. See DOI: 10.1039/d0sc06970a

‡ These authors contributed equally to this work.

temperature, pH and ionic strength, which is fundamental for biomedical applications.[11]

The first examples of $ONOO^-$ generators exclusively controlled by light stimuli were reported by Nakagawa and Miyata almost a decade ago.[12] However, they require poorly biocompatible and scarcely tissue penetrating UVA light for their activation. Therefore, the development of $ONOO^-$ photoprecursors operating with more biocompatible and highly tissue penetrating visible or near infrared (NIR) light is very challenging in view of bio-applications. Very recently, Wang *et al.* reported a molecular construct able to generate $ONOO^-$, as a result of tandem cascade reactions, and to emit green fluorescence upon excitation with visible violet light.[13] The large two-photon absorption cross section of this compound allows also its activation through two-photon excitation in the NIR region.[13]

In this paper we report the design, synthesis, photochemical characterization and biological evaluation of a $ONOO^-$ generator, the molecular hybrid **BPT-NO** (Scheme 1), activatable with single photon red light excitation and which also offers the additional advantage of red fluorescence emission, a useful tool for its cellular tracking. It consists of benzophenothiazine as a suitable light-harvesting antenna, joined to an *N*-nitroso appendage through a flexible spacer. Excitation of this molecular construct with 670 nm light leads to the generation of $ONOO^-$ and produces the analogue non-nitrosate derivative **BPT** as the main stable photoproduct, through the mechanism proposed in Scheme 1 and discussed later.

Results and discussion

Rational design and syntheses

The design and fabrication of photoactivatable $ONOO^-$ generators is not an easy task, as proven by the scarcity of $ONOO^-$ photoprecursors developed to date.[12,13] In fact, since $ONOO^-$ is the result of a very fast reaction between $^{\bullet}NO$ and $O_2^{\bullet-}$, these two species need to be simultaneously generated under light input from suitable chromogenic units. The hybrid **BPT-NO** was inspired by the merging of two different findings: (i) our recently developed $^{\bullet}NO$ photodonors based on green-light antennae covalently linked to the same *N*-nitroso unit of **BPT-NO**;[14] (ii) the recent studies by Peng *et al.* demonstrating that the same phenothiazine unit of **BPT-NO** is a suitable photogenerator of $O_2^{\bullet-}$ under red light excitation.[15] In particular, $^{\bullet}NO$ release from our $^{\bullet}NO$ photodonors proceeds through a mechanism involving an intramolecular photoinduced electron transfer from the nitroso appendage to the excited state (*i.e.* singlet or triplet) of the light-harvesting antennae;[14] on the other hand, the phenothiazine-based system of Peng *et al.* generates $O_2^{\bullet-}$ *via* an intermolecular photoinduced electron transfer involving the lowest triplet state of the red-absorbing chromophore and the molecular oxygen.[15] On the basis of these considerations we thought that the hybrid **BPT-NO** may, in principle, exploit the red excitation energy to trigger the $^{\bullet}NO$ release from the *N*-nitroso unit through a mechanism similar to that reported for other molecular hybrids[13] and, at the same time, produce $O_2^{\bullet-}$ analogously to what was already reported for the benzophenothiazine derivatives.[15]

BPT-NO and its analogue non-nitrosate derivative **BPT**, as a suitable model compound, were synthesized according to the procedures reported in the ESI.† They involve at first the synthesis of the *N*-nitroso and the related non-nitrosate appendage followed by their condensation with the phenothiazine scaffold through an amide linkage.

Spectroscopic and photochemical properties

Fig. 1 shows the UV-Vis spectroscopic features of **BPT-NO** in phosphate buffer (PB) : MeOH (1 : 1 v/v), where the molecular hybrid dissolves quite well. The absorption spectrum is dominated by the benzophenothiazine chromophore, with an intense band with a maximum at 670 nm and extending into the whole red region.[15,16] The fluorescence emission spectrum shows the typical band arising from the benzophenothiazine fluorogenic center, with a maximum at 700 nm and extending up to the near infrared region.[15,16] The fluorescence quantum yield is $\Phi_f = 0.024$ and the related fluorescence decay (see the

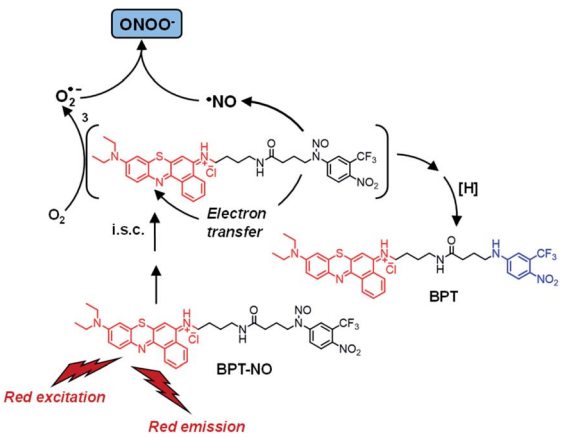

Scheme 1 Proposed molecular mechanism leading to the generation of $ONOO^-$ and the main stable photoproduct **BPT** upon red light excitation of the molecular hybrid **BPT-NO**.

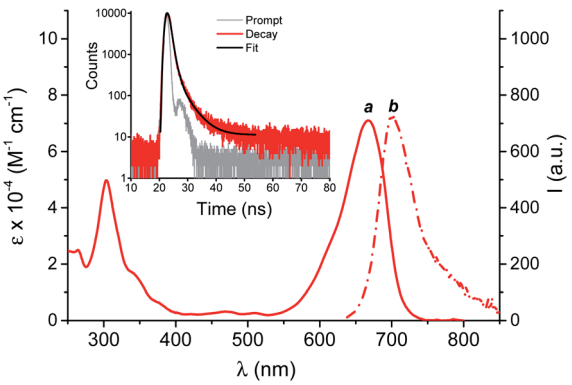

Fig. 1 Absorption (a) and fluorescence emission (b) (λ_{exc} = 620 nm) spectra of a solution of **BPT-NO**. The inset shows the fluorescence decay and the related fitting of the same solutions recorded at λ_{exc} = 455 nm and λ_{em} = 710 nm; PB : MeOH (1 : 1 v/v); T = 25 °C.

inset of Fig. 1) exhibits a dominant component (*ca.* 92%) with a lifetime $\tau_f = 0.90$ ns.

Irradiation of a N_2-saturated solution of **BPT-NO** with red light leads to the absorption spectral changes illustrated in Fig. 2A. They show bleaching of the main absorption bands in the visible and UV region, and the formation of a new absorption band at 390 nm accompanied by the presence of isosbestic points at 583 and 324 nm, which are indicative of the occurrence of a quite clean photochemical reaction. Such a spectral evolution is in excellent agreement with the formation of the non-nitrosate compound **BPT** characterized by a lower molar absorptivity in the Vis and UV regions and by the characteristic band at 390 nm arising from the push–pull character of the nitroaniline moiety[17] (Fig. S1†). This band is suppressed in **BPT-NO** because of the presence of the electron withdrawing nitroso group attached to the amino functionality. HPLC analysis carried out with the authentic model compound **BPT** as a reference confirmed it to be the only stable photoproduct (Fig. S2†). The absorption profile observed in air-equilibrated solution was identical in nature but slower when compared to that observed under anaerobic conditions (see the inset of Fig. 2A). This finding provides an unambiguous indication that the photoreactivity of **BPT-NO** is more likely mediated by a long-lived excited triplet state rather than the singlet one. This proposal accords well with the values of Φ_f and τ_f found for the non-nitrosate compound **BPT** (Fig. S3†) which were identical to those of **BPT-NO**. This rules out any other deactivation process from the excited singlet state of **BPT-NO** competitive with fluorescence and intersystem crossing (i.s.c.) to the triplet state. Furthermore, the short τ_f, makes any diffusional quenching of the excited singlet state by molecular oxygen non-competitive with the singlet decay.

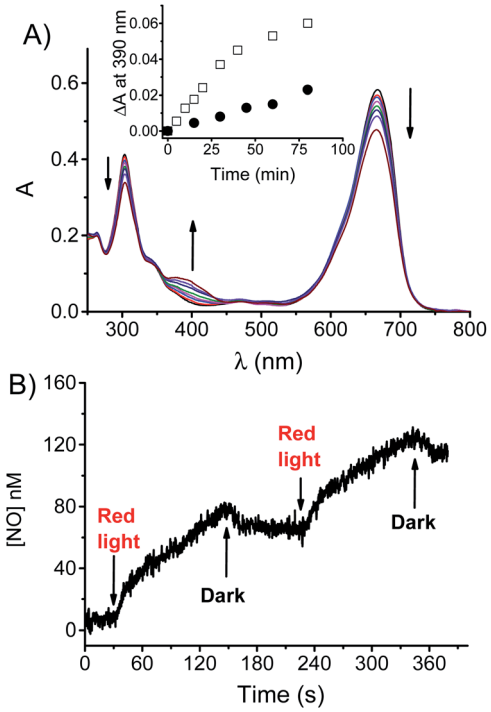

Fig. 2 (A) Absorption spectral changes observed upon exposure of a N_2-saturated solution of BPT-NO to red light at $\lambda_{exc} = 670$ nm for different time intervals (0–80 min). The arrows indicate the course of the spectral profile with the illumination time. The insets show the absorbance changes at $\lambda = 390$ nm in N_2-saturated (□) and air-equilibrated (●) solution. (B) NO release profile observed for a solution of BPT-NO upon alternate cycles of red light ($\lambda_{exc} = 670$ nm) and dark. [BPT-NO] = (8.5 μM); PB : MeOH (1 : 1 v/v), $T = 25$ °C.

Formation of **BPT** as the only stable photoproduct clearly indicates the occurrence of ˙NO photorelease from **BPT-NO** upon red light excitation. This was demonstrated by the direct detection of this radical through an amperometric technique using an ultrasensitive ˙NO electrode. Fig. 2B shows that ˙NO release by **BPT-NO** takes place exclusively under stimuli of red light, stops in the dark, and restarts as the red light is turned on again. Since the benzophenothiazine chromophore is the sole antenna absorbing the red excitation light, loss of ˙NO from the *N*-nitroso moiety must necessarily involve an electronic communication between these two components. Population of the *N*-nitroso appendage by photoinduced energy transfer from the excited benzophenothiazine is, of course, not possible because it is highly endergonic.[18] Therefore, uncaging of ˙NO from **BPT-NO** seems to be triggered by a photoinduced electron transfer from the *N*-nitrosoaniline-derivative moiety, as an electron donor, to the excited triplet state of benzophenothiazine, as an electron acceptor, similarly to what was recently observed for a doxorubicin molecular hybrid.[14a] According to literature, oxidation of the *N*-nitroso functionality strongly encourages the ˙NO detachment.[14,19] Our proposal is also supported by the negative free energy value for the photoinduced triplet electron transfer processes, $\Delta G \sim 0.2$ eV, estimated using the Rehm–Weller equation:[20]

$$\Delta G = e[E_{ox} - E_{red}] - E_T$$

where E_{ox} is the half-wave potential for one-electron oxidation of the electron-donor unit, *ca.* 1 eV *vs.* NHE,[21] E_{red} is the half-wave potential for one-electron reduction of the electron-acceptor unit, *ca.* −0.2 eV *vs.* NHE,[22] and E_T is the average energy of the lowest excited triplet states of the light harvesting centers, *ca.* 1.4 eV.[23]

The proposed photoinduced intramolecular electron transfer is strongly facilitated by the proximity of the electron donor and electron acceptor units due to the U-shaped conformation adopted by **BPT-NO**, as confirmed by molecular dynamics simulations (Fig. S4†).

Taken together, all these results account well for the ˙NO release mechanism proposed in Scheme 1. ˙NO release after triplet mediated electron transfer involves, of course, the generation of an anilino radical derivative after a back electron transfer. This species is strongly stabilized by the presence of the two electron drawing nitro and trifluoromethyl groups. Besides, it is expected to be basically insensitive to the presence of oxygen and to evolve to the stable photoproduct **BPT**, after i.s.c. and H-transfer from the solvent, the latter typically observed for the other *N*-nitrosamine after loss of ˙NO.[14,24]

Quenching of the lowest triplet state by molecular oxygen usually occurs through type I or type II mechanisms.[7,25] The

former leads to $O_2^{\bullet-}$ through intermolecular electron transfer and the latter generates $^1O_2$ through a collisional energy transfer process.[7,25] As outlined above, the benzophenothiazine unit integrated in the structure of **BPT-NO** was appropriately chosen due to its capability to generate $O_2^{\bullet-}$ under red light excitation.[15] In this case, if $O_2^{\bullet-}$ is generated simultaneously to $^{\bullet}NO$, it is expected to react with the latter at a diffusion-controlled rate to produce $ONOO^-$.[1]

Generation of $ONOO^-$ was demonstrated by experiments carried out in the presence of fluorescein-boronate (Fl-B), a very selective and sensitive probe for $ONOO^-$ recently developed by Radi *et al.*[26] Fl-B is weakly fluorescent but it is rapidly ($k \sim 10^6$ M^{-1} s^{-1}) and effectively (yield = 99%) oxidized by $ONOO^-$, liberating the highly fluorescent fluorescein.[25] Fig. 3 shows the appearance of the typical fluorescence excitation and emission spectra of fluorescein with λ_{max} = 490 nm and 520 nm, respectively, upon irradiation of an air-equilibrated solution of **BPT-NO**. In contrast, negligible fluorescence emission was observed when **BPT-NO** was irradiated under N_2-saturated conditions where the $O_2^{\bullet-}$ required for the $ONOO^-$ is, of course, not generated (inset of Fig. 3).§ Besides, very low emission increase was observed in the case of the model compound **BPT** as a suitable control (see the inset of Fig. 3), according to the absence of $^{\bullet}NO$ photorelease occurring in this compound. This low, but no negligible emission increase in the case of this compound might arise from the very slow oxidation ($k \sim$ 1–2 M^{-1} s^{-1}) of Fl-B by the H_2O_2 (ref. 25) derived by the slow dismutation of $O_2^{\bullet-}$, which in **BPT** is expected to be produced analogously to **BPT-NO**, but not consumed in the reaction with $^{\bullet}NO$. This hypothesis was confirmed by using the dihydrorhodamine 123 probe which is non-fluorescent but becomes strongly green fluorescent after reaction with $O_2^{\bullet-}$ (Fig. S5†).[15a] Quantitative comparison between the amount of the photoproduct **BPT** and the fluorescein formed in the early stage of the photoreaction was then performed by HPLC which revealed the % (mol mol^{-1}) for these compounds to be 9.8 ± 1.3 and 7.4 ± 1.1, respectively. Since $ONOO^-$ quantitatively oxidizes Fl-B to fluorescein, this finding suggests that NO is produced only slightly in excess with respect to $O_2^{\bullet-}$ of *ca.* 1.3 fold (9.8/7.4).

Additional confirmation for the formation of $ONOO^-$ was provided by analysis of the nitrite (NO_2^-) formed after irradiation and its quantitative comparison with the only stable photoproduct **BPT**. In fact, in the absence of other reactive species, $^{\bullet}NO$ is almost quantitatively oxidized to NO_2^- but not to NO_3^- by molecular oxygen.[27] Therefore, in such a case NO_2^- and **BPT** are expected to be found in an equimolar ratio. NO_2^- was detected by using both the very sensitive spectrofluorimetric and spectrophotometric assays based on 2,3-diaminonaphthalene (DAN)[28] and Griess[29] reactants, respectively. Fig. 4 shows the characteristic well-structured fluorescence emission and excitation spectra of the highly fluorescent 2,3-diaminonaphthotriazole (DANT) formed after reaction of DAN with NO_2^-, only in the irradiated sample and with intensity strictly dependent on the irradiation time.

Quantitative comparison between NO_2^- and **BPT** was then carried out in the early stage of the photoreaction by the Griess assay. The inset of Fig. 4 clearly shows that the amount of NO_2^- was much lower than that of **BPT**, with the related % (mol mol^{-1}) being 3.2 ± 0.5 and 9.6 ± 1.4, respectively. This result in good agreement with the generation of $O_2^{\bullet-}$, which rapidly converts the $^{\bullet}NO$ photogenerated into $ONOO^-$ before it is slowly oxidized to NO_2^- by molecular oxygen. This view was well supported by the NO_2^- analysis performed after treating the

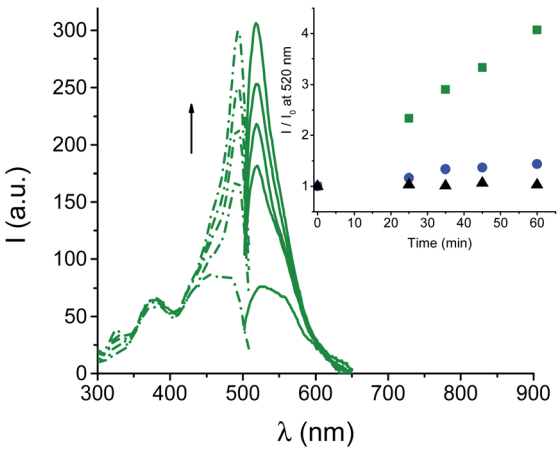

Fig. 3 Fluorescence emission (solid) and excitation (dotted) spectra recorded at λ_{exc} = 492 nm and λ_{em} = 520 nm, respectively, observed upon irradiation with red light at λ_{exc} = 670 nm of an air-equilibrated solution **BPT-NO** in the presence of Fl-B. The arrow indicates the course of the spectral profile with the illumination time. The inset shows the fluorescence emission increase observed at λ = 520 nm in the case of the air-equilibrated solutions of **BPT-NO** (■) and the model compound **BPT** (●), and a N_2-saturated solution of **BPT-NO** (▲) (I and I_0 represent the fluorescence intensities after and before irradiation, respectively). [**BPT-NO**] = [Fl-B] = [**BPT**] = (25 μM); PB : MeOH (1 : 1 v/v); T = 25 °C.

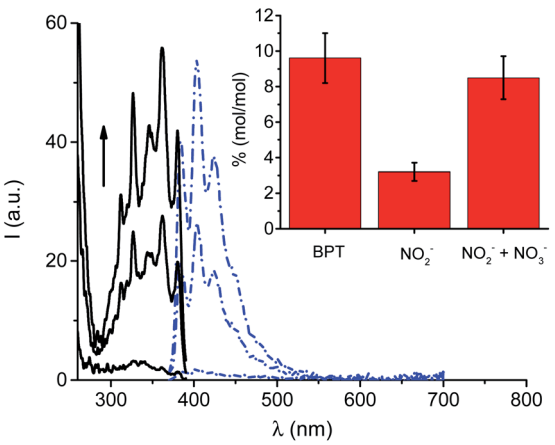

Fig. 4 Fluorescence excitation (solid) and emission (dotted) spectra obtained after fluorimetric DAN assay of solutions of **BPT-NO** (8.5 μM) after 0, 30 and 60 min of irradiation (from bottom to top) with red light at λ_{exc} = 670 nm. The emission wavelength for the excitation spectra was 410 nm whereas the excitation wavelength for the emission spectra was 360 nm. The inset shows the % (mol mol^{-1}) of the photoproduct **BPT** and the respective amounts of NO_2^- and NO_2^- + NO_3^- observed after 30 min of irradiation; PB : MeOH (1 : 1 v/v); T = 25 °C.

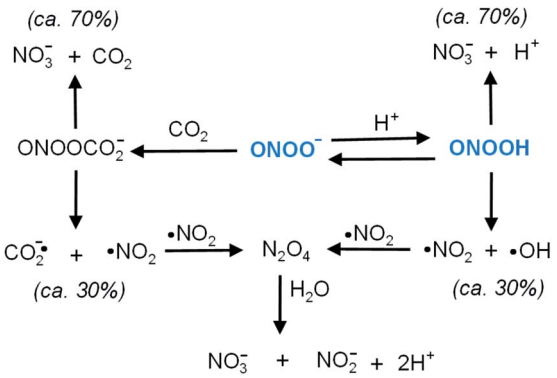

Scheme 2 Typical decomposition mechanism of $ONOO^-$.

irradiated mixture of **BPT-NO** with VCl_3. In fact, $ONOO^-$ leads to a large amount of nitrate (NO_3^-) according to the well-known decomposition pathways of $ONOO^-$ and its conjugate acid ONOOH recalled in Scheme 2, for the sake of clarity. The inset of Fig. 4 shows that the total NO_2^- detected after treatment of the irradiated solution with VCl_3, which is able to convert NO_3^- into NO_2^-,[30] remarkably increased reaching a value very close to that of the photoproduct **BPT**.

A specific point that needs to be clarified is related to the photodegradation mechanism proposed in Scheme 1. The type I reaction involved in the generation of $O_2^{\bullet-}$ involves, of course, the formation of a benzophenothiazine-centered radical cation, which is expected to evolve to products besides **BPT**. Therefore, at first sight, the observation of **BPT** as the sole stable product of photolysis can seem quite surprising. A possible hypothesis to explain this finding might consist of a typical deprotonation of the benzophenothiazine-centered radical cation, leading to neutral radical species which would restore the starting benzophenothiazine chromophore by H-transfer from the solvent.

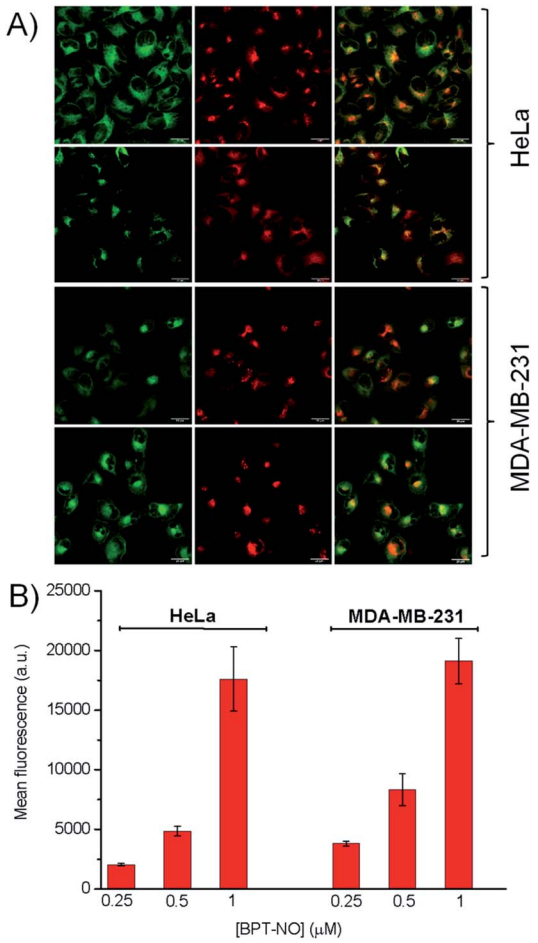

Fig. 5 (A) Confocal images of cancer cells incubated for 2 h with 0.5 μM **BPT-NO** (red fluorescence). The cells are stained with BODIPY® FL C5-ceramide (Golgi apparatus, top panels) or ER-Tracker™ Green (endoplasmic reticulum, bottom panels) (green fluorescence). Overlays of red and green fluorescence are shown in the right of each panel. Scale bar = 20 μm. (B) Cellular uptake of different concentrations of **BPT-NO** measured by flow cytometry after 2 h incubation.

Cell internalization and toxicity

The biological activity of **BPT-NO** was evaluated with two different cancer cell lines, HeLa (derived from a human cervix carcinoma) and MDA-MB-231 (derived from a human breast carcinoma). The intracellular localization of internalized **BPT-NO** was determined by confocal fluorescence microscopy after 2 h incubation of cell monolayers. Fifteen minutes before completing the incubation, the cells were stained with either BODIPY® FL C5-ceramide or ER-Tracker™ Green used as markers for Golgi apparatus and endoplasmic reticulum, respectively. Fluorescence images of the cells were then acquired using 633 nm and 488 nm lasers as excitation sources for **BPT-NO** and organelle markers, respectively. The overlapping of green (organelle markers) and red fluorescence (**BPT-NO**) (Fig. 5A) shows clear-cut evidence for the localization of the molecular hybrid in the endoplasmic reticulum and Golgi apparatus of HeLa and MDA-MB-231 cells. In contrast, poor localization in lysosomes and mitochondria was observed (Fig. S6†). Flow cytometry analysis showed that the intracellular uptake was very efficient and strictly dependent on the concentration of **BPT-NO** (Fig. 5B).

To assess the efficacy of the molecular hybrid as a phototherapeutic agent, the cancer cells were incubated for 2 h with increasing concentrations of **BPT-NO**, and either kept in the dark or irradiated with very low doses of red light (1 J cm^{-2}). Fig. 6 shows that no relevant toxicity was observed in the dark in a concentration range below 2 μM. In contrast, in the same concentration range a remarkable decrease of cell viability was observed, with both cell lines upon irradiation, with the loss of cell viability being strictly dependent on the concentration of **BPT-NO**. A remarkable point which deserves to be stressed is that the strong phototoxic effects are induced by using very low concentrations of the molecular hybrid combined with very low doses of red light irradiation. This is in excellent agreement with the high toxicity of the $ONOO^-$ and its secondary free radical species, as also confirmed by the lower phototoxic effects displayed by the model compound **BPT** (Fig. S7†).

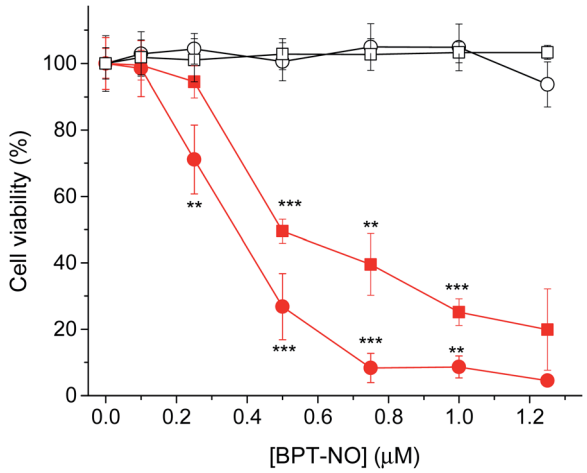

Fig. 6 Cell viability of HeLa (circles) and MDA-MB-231 (square) cancer cells incubated for 2 h with **BPT-NO** and either kept in the dark (open symbols) or irradiated (filled circles) with red light at a fluency of 1 J cm^{-2} (40 mW cm^{-2} for 25 s). *p < 0.05; **p < 0.1; ***p < 0.001.

Conclusions

In summary, we have developed a novel molecular hybrid which represents a rare example of an $ONOO^-$ generator exclusively controlled by visible light. The present compound offers remarkable advantages compared with the few existing $ONOO^-$ photodonors such as (i) $ONOO^-$ generation triggered by highly biocompatible and tissue penetrating single photon red light, corresponding to an improvement of *ca.* 250 nm in terms of excitation wavelength; (ii) very high extinction coefficient in the red region, allowing the absorption of red photons even in a very low concentration range; (iii) satisfactory red fluorescence, useful for cellular tracking. Besides, the only generated stable photoproduct does not suffer from the disadvantage of undergoing undesired reactions with $ONOO^-$. Finally, it is very important to underline that $^{\bullet}NO$ and $O_2^{\bullet-}$, responsible for the formation of $ONOO^-$, are generated in comparable amounts, with the former being in slight excess with respect to the latter. It is well known that in biological systems, while oxidative pathways involving a direct reaction with $ONOO^-$ are not altered, oxidative processes initiated by the $^{\bullet}NO_2/CO_3^{\bullet-}/^{\bullet}OH$ secondary free radicals, formed from the small fraction of spontaneous decomposition of $ONOO^-$ (see Scheme 2), are inhibited by an excess production of either $^{\bullet}NO$ or $O_2^{\bullet-}$.[31] On the basis of these results we expect that **BPT-NO** can open up intriguing prospects in chemical and biomedical research for studies where precise and spatiotemporally concentrations of $ONOO^-$ are required.

Author contributions

M. F. and C. P. carried out the synthesis, C. P. and A. F. performed the spectroscopic and photochemical experiments, B. R. performed the HPLC analysis, F. S. performed the molecular dynamics calculations, L. M. performed the fluorescence microscopy analysis, F. M. and E. R. performed the cell toxicity experiments, L. L. supervised the synthesis and contributed to the discussion and editing, R. F. contributed to the discussion and editing, A. G. conceived the synthesis and contributed to the discussion, S. S. devised the work, coordinated the experiments and wrote the paper.

Conflicts of interest

We have no conflict of interest to declare.

Acknowledgements

We thank AIRC – Italian Association for Cancer Research (IG-19859) for financial support.

Notes and references

§ Experiments performed in O_2-saturated solution revealed that the amount of $ONOO^-$ photogenerated is *ca.* 25% smaller than that observed in air-equilibrated solution. This result is in good agreement with the mechanism proposed and involved the long-lived excited triplet state of **BPT-NO** as the key intermediate in the photodecomposition. In fact, an increase of the O_2 concentration on one hand could lead to an increase of the concentration of $O_2^{\bullet-}$ *via* a bimolecular reaction with the triplet state; on the other hand it is expected to increase the triplet quenching efficiency, reducing the amount of NO generated by a unimolecular reaction from this excited state.

1 (*a*) N. V. Blough and O. C. Zafiriou, *Inorg. Chem.*, 1985, **24**, 3502–3504; (*b*) R. Kissner, T. Nauser, P. Bugnon, P. G. Lye and W. H. Koppenol, *Chem. Res. Toxicol.*, 1997, **10**, 1285–1292; (*c*) S. Goldstein and G. Czapski, *Free Radical Biol. Med.*, 1995, **19**, 505–510.

2 R. Radi, G. Peluffo, M. N. Alvarez, M. Naviliat and A. Cayota, *Free Radical Biol. Med.*, 2001, **30**, 463–488.

3 G. Ferrer-Sueta and R. Radi, *ACS Chem. Biol.*, 2009, **4**, 161–177.

4 (*a*) R. M. Uppu and W. A. Pryor, *J. Am. Chem. Soc.*, 1999, **121**, 9738–9739; (*b*) G. Merényi, J. Lind, S. Goldstein and G. Czapski, *Chem. Res. Toxicol.*, 1998, **11**, 712–713.

5 (*a*) G. Ferrer-Sueta, N. Campolo, M. Trujillo, S. Bartesaghi, S. Carballal, N. Romero, B. Alvarez and R. Radi, *Chem. Rev.*, 2018, **118**, 1338–1408; (*b*) S. Bartesaghia and R. Radi, *Redox Biol.*, 2018, **14**, 618–625; (*c*) R. Radi, *J. Biol. Chem.*, 2013, **288**, 26464–26472.

6 (*a*) C. Szabó, H. Ischiropoulos and R. Radi, *Nat. Rev. Drug Discovery*, 2007, **6**, 662–679; (*b*) J. S. Beckman and W. H. Koppenol, *Am. J. Physiol.*, 1996, **271**, 1424–1437; (*c*) N. Hogg, V. M. Darley-Usmar, M. T. Wilson and S. Moncada, *Biochem. J.*, 1992, **291**, 419–424.

7 (*a*) A. P. Castano, P. Mroz and M. R. Hamblin, *Nat. Rev. Cancer*, 2006, **6**, 535–545; (*b*) J. P. Celli, B. Q. Spring, I. Rizvi, C. L. Evans, K. S. Samkoe, S. Verma, B. W. Pogue and T. Hasan, *Chem. Rev.*, 2010, **12**, 2795–2838.

8 (*a*) H. Gunaydin and K. N. Houk, *Chem. Res. Toxicol.*, 2009, **22**, 894–898; (*b*) R. Radi, *Proc. Natl. Acad. Sci. U. S. A.*, 2004, **101**, 4003–4008.

9 (*a*) M. M. Gottesman, *Annu. Rev. Med.*, 2002, **53**, 615–627; (*b*) N. A. Colabufo, F. Berardi, M. Contino, M. Niso and R. Perrone, *Curr. Top. Med. Chem.*, 2009, **9**, 119–129.

10 (*a*) A. Fraix, C. Conte, E. Gazzano, C. Riganti, F. Quaglia and S. Sortino, *Mol. Pharmaceutics*, 2020, **17**, 2135–2144; (*b*) C. Riganti, E. Miraglia, D. Viarisio, C. Costamagna, G. Pescarmona, D. Ghigo and A. Bosia, *Cancer Res.*, 2005, **65**, 516–525; (*c*) K. Chegaev, A. Fraix, E. Gazzano, G. E. F. Abd-Ellatef, M. Blangetti, B. Rolando, S. Conoci, C. Riganti, R. Fruttero, A. Gasco and S. Sortino, *ACS Med. Chem. Lett.*, 2017, **8**, 361–365.

11 (*a*) S. Sortino, *J. Mater. Chem.*, 2012, **22**, 301–318; (*b*) Topics in Curr. Chem., *Light-responsive nanostructured systems for applications in nanomedicine*, ed. S. Sortino, 2016, vol. 370; (*c*) S. Swaminathan, J. Garcia-Amoròs, A. Fraix, N. Kandoth, S. Sortino and F. M. Raymo, *Chem. Soc. Rev.*, 2014, **43**, 4167–4178.

12 (*a*) N. Ieda, H. Nakagawa, T. Peng, D. Yang, T. Suzuki and N. Miyata, *J. Am. Chem. Soc.*, 2012, **134**, 2563–2568; (*b*) N. Ieda, H. Nakagawa, T. Horinouchi, T. Peng, D. Yang, H. Tsumoto, T. Suzuki, K. Fukuhara and M. Naoki, *Chem. Commun.*, 2011, **47**, 6449–6451.

13 J. Sun, X. Cai, C. Wang, K. Du, W. Chen, F. Feng and S. Wang, *J. Am. Chem. Soc.*, 2021, **143**, 868–878.

14 (*a*) A. Fraix, C. Parisi, M. Failla, K. Chegaev, F. Spyrakis, L. Lazzarato, R. Fruttero, A. Gasco and S. Sortino, *Chem. Commun.*, 2020, **56**, 6332–6335; (*b*) C. Parisi, M. Failla, A. Fraix, B. Rolando, E. Gianquinto, F. Spyrakis, E. Gazzano, C. Riganti, L. Lazzarato, R. Fruttero, A. Gasco and S. Sortino, *Chem.–Eur. J.*, 2019, **25**, 11080–11084; (*c*) C. Parisi, A. Fraix, S. Guglielmo, F. Spyrakis, B. Rolando, L. Lazzarato, R. Fruttero, A. Gasco and S. Sortino, *Chem.–Eur. J.*, 2020, **26**, 13627–13633; (*d*) C. Parisi, M. Failla, A. Fraix, A. Rescifina, B. Rolando, L. Lazzarato, V. Cardile, A. C. E. Graziano, R. Fruttero, A. Gasco and S. Sortino, *Bioorg. Chem.*, 2019, **85**, 18–22.

15 (*a*) M. Li, J. Xia, R. Tian, J. Wang, J. Fan, J. Du, S. Long, X. Song, J. W. Foley and X. Peng, *J. Am. Chem. Soc.*, 2018, **140**, 14851–14859; (*b*) B. Gurram, M. Li, M. Li, K. H. Gebremedhin, W. Sun, J. Fan, J. Wang and X. Peng, *J. Mater. Chem. B*, 2019, **7**, 4440–4450.

16 S. Verma, U. W. Sallum, H. Athar, L. Rosenblum, J. W. Foley and T. Hasan, *Photochem. Photobiol.*, 2009, **85**, 111–118.

17 (*a*) E. B. Caruso, S. Petralia, S. Conoci, S. Giuffrida and S. Sortino, *J. Am. Chem. Soc.*, 2007, **129**, 480–481; (*b*) S. Conoci, S. Petralia and S. Sortino, EP 2051935A1/*US Pat.*20090191284, 2006; (*c*) S. Sortino, *Chem. Soc. Rev.*, 2010, **39**, 2903–2913.

18 The lowest excited singlet state of the *N*-nitroso unit is *ca.* 1.5 eV higher than the lowest excited singlet state of the benzophenothazine chromophore.

19 (*a*) N. Ieda, Y. Hotta, N. Miyata, K. Kimura and H. Nakagawa, *J. Am. Chem. Soc.*, 2014, **136**, 7085–7091; (*b*) H. Okuno, N. Ieda, Y. Hotta, M. Kawaguchi, K. Kimura and H. Nakagawa, *Org. Biomol. Chem.*, 2017, **15**, 2791–2796.

20 D. Rehm and A. Weller, *Isr. J. Chem.*, 1970, **8**, 259–262.

21 (*a*) M. Jonsson, J. Lind, T. E. Eriksen and G. Merényi, *J. Am. Chem. Soc.*, 1994, **116**, 1423–1427; (*b*) Y. L. Chow, *Acc. Chem. Res.*, 1973, **6**, 354–360.

22 T. Ohno and N. N. Lictin, *J. Am. Chem. Soc.*, 1980, **102**, 4636–4643.

23 M. Montalti, A. Credi, L. Prodi and M. T. Gandolfi, *Handbook of Photochemistry*, CRC Press, Boca Raton, 3rd edn, 2006.

24 (*a*) H. He, Y. Xia, Y. Qi, H.-Y. Wang, A. Wang, J. Bao, Z. Zhang, F.-G. Wu, H. D. Chen, D. Yang, X. Liang, J. Chen, S. Zhou, X. Liang, X. Qian and Y. Yang, *Bioconjugate Chem.*, 2018, **29**, 1194–1198; (*b*) H. He, Z. Ye, Y. Xiao, W. Yang and Y. Yang, *Anal. Chem.*, 2018, **90**, 2164–2169.

25 (*a*) I. J. McDonald and T. Doughery, *J. Porphyrins Phthalocyanines*, 2001, **5**, 105; (*b*) T. Hasan, A. C. E. Moor and B. Ortel, *Cancer Medicine*, Decker BC Inc., Hamilton, Ontario, Canada, 5th edn, 2000.

26 N. Riosa, L. Piacenza, M. Trujillo, A. Martíneza, V. Demichelia, C. Prolo, M. N. Álvareza, G. V. Lópezb and R. Radi, *Free Radical Biol. Med.*, 2016, **101**, 284–295.

27 L. J. Ignarro, J. M. Fukuto, J. M. Griscavage, N. E. Rogers and R. E. Byrns, *Proc. Natl. Acad. Sci. U. S. A.*, 1993, **90**, 8103–8107.

28 T. P. Misko, R. J. Schilling, D. Salvemini, W. M. Moore and M. G. Currie, *Anal. Biochem.*, 1993, **214**, 11–16.

29 N. S. Bryan and M. B. Grisham, *Free Radical Biol. Med.*, 2007, **43**, 645–657.

30 K. M. Miranda, M. G. Espey and D. A. Wink, *Nitric Oxide*, 2001, **5**, 62–71.

31 D. Jourd'heuil, F. L. Jourd'heuil, P. S. Kutchukian, R. A. Musah, D. A. Winki and M. B. Grisham, *J. Biol. Chem.*, 2001, **276**, 28799–28805.